JOURNAL OF SOLID STATE CHEMISTRY 109, 321–332 (1994)

The Effect of Thallium and Oxygen Stoichiometry on Structure and T_c in Tl-2201 and Tl-2212

C. Ström,[1] S.-G. Eriksson, and L.-G. Johansson

Department of Inorganic Chemistry, Chalmers University of Technology and University of Göteborg, S-412 96 Göteborg, Sweden

and

A. Simon, H. J. Mattausch, and R. K. Kremer

Max-Planck-Institut für Festkörperforschung, 7000 Stuttgart 80, Germany

Received January 26, 1993; in revised form August 2, 1993; accepted August 3, 1993

By a novel method we have prepared the high-T_c superconductors $Tl_{2-x}Ba_2CuO_{6-d}$ Tl-2201) and $Tl_{2-x}Ba_2CaCu_2O_{8-d}$ (Tl-2212) in a reproducible way with respect to purity, thallium and oxygen content, crystal structure, and superconducting properties. The changes in structure induced by changes in thallium or oxygen content were studied by X-ray and neutron powder diffraction techniques. Tl-2201 crystallizes in either the tetragonal or orthorhombic system, and both forms can be made superconducting. The detailed atomic order in the Tl_2O_4 layers seems to be determined by the thallium as well as by the oxygen content. A high thallium and oxygen content stabilizes the orthorhombic form. Tl-2212 has tetragonal symmetry irrespective of thallium or oxygen content. In samples low in thallium content no single layer thallium compounds are formed, the thallium deficiency being accommodated as statistically distributed vacancies in the Tl_2O_4 layers. The oxygen content is the main factor in determining T_c in Tl-2201 and Tl-2212. Low thallium content promotes higher T_c's, whereas addition of oxygen to the as-prepared samples decreases T_c. The *c*-axis length of Tl-2201 decreases by about 0.06 Å when annealed in oxygen at 300°C. In Tl-2212 the shortening of the *c*-axis length is about 0.08 Å for the same annealing treatment. The change in *c*-axis length and the atom displacements, in particular in the Tl-2212 system, can be explained in terms of a charge redistribution as for the Y-123 system. An increase in oxygen content leads to a shift of Ba^{2+} toward the Tl_2O_4 layers, and to an increase in the CuO_2 plane puckering as expected from an increase in hole concentration in the CuO_2 planes.

1. INTRODUCTION

The structure and superconducting properties of layered cuprates have been discussed in detail (1, 2). A relation between T_c and hole concentration in the CuO_2 planes has been established for a large number of systems via, e.g., chemical analysis and Hall effect measurements (3). The hole concentration depends not only on chemical composition but also on the detailed atomic order such as the CuO_3 chain ordering in Y-123 (4–9).

The thallium cuprates together with the new mercury cuprates comprise the compounds with the highest T_c values known today (10–13). $Tl_{2-x}Ba_2CuO_{6-d}$ (Tl-2201) and $Tl_{2-x}Ba_2CaCu_2O_{8-d}$ (Tl-2212) are the subjects of many investigations (13–24). However, a comparison of superconducting properties of thallium cuprates prepared in different laboratories is of somewhat limited use as T_c values cover a wide range due to nonidentical preparative conditions. Tl-2201 seems particularly sensitive to stoichiometric variations and the whole range from a nonsuperconductor to a 90 K superconductor has been found.

The oxygen and thallium content as well as the detailed atomic order in the Tl_2O_4 layers of thallium cuprates determines their superconducting properties (24–30). They can be changed by annealing in argon, oxygen, or hydrogen atmosphere (25, 31–34). To explain the variable properties of the Tl-based superconductors a number of arguments have been offered such as Tl vacancies in the Tl_2O_4 layers (14, 35–38), presence of additional (interstitial) oxygen in the Tl_2O_4 layers (14, 26, 39–41), and the occurrence of Tl in an oxidation state less than +3 (19, 30, 36, 42–47). Moreover, in Tl-2212 a partial occupation of the Ca site by Tl occurs (28, 29, 48, 49). The hole concentration in the CuO_2 layers of thallium cuprates is therefore difficult to estimate (42, 44, 50–52). It is likely that not only the oxygen and thallium content determine the hole concentration in the CuO_2 planes, but that "self-doping" occurs due to an overlap of the Tl-6*s* and Cu-$d_{x^2-y^2}$ bands, i.e., an intrinsic redox process. Any distortion of the Tl_2O_4 layers strongly influences the energy of the Tl-6*s* bands and therefore the overlap with the Cu-*d* bands.

Using an earlier-developed route (53–54) we prepared

[1] To whom correspondence should be addressed.

0022-4596/94 $6.00

a series of thallium cuprates to be investigated by thermogravimetry, electrical measurements, and X-ray and neutron diffraction. The samples exhibit reproducible results concerning purity, crystal structure, and T_c. Questions such as the influence of thallium and oxygen content upon the polymorphism of tetragonal–orthorhombic Tl-2201 and superconducting properties as well as the importance of the detailed atomic order in the Tl_2O_4 layers are addressed. Also the concept of charge transfer is highlighted.

2. EXPERIMENTAL

2.1. Synthesis

Samples weighing about 10 g were prepared from mixtures of Tl_2O_3, $Ba(OH)_2 \cdot H_2O$, CaO, and $Cu(NO_3)_2 \cdot nH_2O$, always in the ratio of cations desired in the final material with no excess of any element. All samples in each series were prepared in the same batch to make the preparative conditions as identical as possible. Before use the starting materials were characterized according to Table 1. The powders, milled in ethanol and thereafter dried in inert atmosphere (N_2), were heat treated by a two-step sintering process according to Table 2. The heating rate in both steps was 180°C/hr, and the temperature was regulated by a controller, Eurotherm 818P, with a temperature stability better than ±0.5°C.

In sintering Step 1 the mixtures were heated in Al_2O_3 crucibles with Al_2O_3 covers. As the starting materials are reactive, this step can be run at low temperature (760°C) with only a limited loss, if any at all, of thallium. As an extra check for thallium loss a well-known amount of Tl_2O_3 was heated at 760°C for 3 hr. No weight loss and no reaction with the container material occur.

In sintering Step 2 pellets were placed in Al_2O_3 crucibles sealed with gold gaskets and cover. They were subsequently centered in small pieces of ceramic tubes and fixed with steel wedges. The gold as well as the wedges expands during heating, and the external pressure exposed on the Al_2O_3 crucible, gold gasket, and cover prevents evaporation from the crucible. There is no sign of substitution of gold into the material or of incorporation of thallium into the gold gasket. From EDX analysis no traces of Al or Au can be detected in the sample.

We have monitored the loss of weight in sintering Step 2, which, if attributed solely to thallium evaporation, is below 0.3% of the total amount of thallium (Tables 3 and 4). The estimated loss of thallium was calculated from the weight loss and the expected molar weight of the product, with an average oxygen content of 5.7 and 7.8 for Tl-2201 and Tl-2212, respectively. Even if the real oxygen content may differ slightly from these values it only affects the calculation to a minor extent. Estimated errors in barium and copper content, concerning the nominal sample composition, are of the sizes stated in Table 1.

As-prepared samples (Series A) were cut in two pieces and one piece was annealed in oxygen (Series B) as stated in Table 2. The annealing reaction was completed when no further change in sample weight occurred, which indicated that equilibrium had been reached with respect to oxygen content. No formation of impurity phases or extrusion of thallium was detected by visual inspection and X-ray analysis in contradiction to other work (42, 44). The oxygen-annealed product had as high crystallinity as the starting material. We present the change in oxygen content on a relative scale (See Tables 3 and 4). The change in oxygen content is determined accurately by weighing the material before and after oxygen annealing (estimated errors in a 5-g batch correspond to ±0.005 oxygen atoms/formula unit). In order to exclude the possibility of a change in thallium content during the annealing procedure, Tl_2O_3 was heated in oxygen at 300°C for 70 hr. No change in weight was observed, indicating a constant thallium content during this annealing step.

The use of a prereacted precursor and a well-controlled ratio of sample-to-container volume in the second sintering step (resulting in nearly identical pressures of O_2 and Tl_2O in different preparations) together with the limited loss of thallium leads to well-defined products. Moreover, the low sintering temperature (860°C in the case of

TABLE 1

Formula	Source	Pretreatment	Characterization
Tl_2O_3	Aldrich, 99.99%	Heated at 300°C for 3 hr	Gravimetric analysis
$Ba(OH)_2\ H_2O$	Sigma, 99.0%	$Ba(OH)_2\ 8H_2O$ dried in vacuum at 70°C for 24 hr ($-7H_2O$)	Gravimetric analysis of Ba as $Ba(CrO_4)$ (s), accuracy ±0.2%
CaO	Merck, PA	Calcination of $CaCO_3$ to CaO at 950°C for 2 hr	Gravimetric analysis
$Cu(NO_3)_2\ nH_2O$	Merck, PA	—	Electrochemical analysis of the copper content, accuracy ±0.2%

TABLE 2

Sample	Starting composition Tl : Ba : Ca : Cu	Sintering		Annealing
		Step 1	Step 2	
A1	1.85 : 2 : 0 : 1	760°C/3 hr	860°C/6 hr	None
A2	1.95 : 2 : 0 : 1	760°C/3 hr	860°C/6 hr	None
A3	2.00 : 2 : 0 : 1	760°C/3 hr	860°C/6 hr	None
B1	1.85 : 2 : 0 : 1	760°C/3 hr	860°C/6 hr	300°C/O_2/70 hr
B2	1.95 : 2 : 0 : 1	760°C/3 hr	860°C/6 hr	300°C/O_2/70 hr
B3	2.00 : 2 : 0 : 1	760°C/3 hr	860°C/6 hr	300°C/O_2/70 hr
A4	1.75 : 2 : 1 : 2	760°C/3 hr	880°C/6 hr	None
A5	1.85 : 2 : 1 : 2	760°C/3 hr	880°C/6 hr	None
A6	2.00 : 2 : 1 : 2	760°C/3 hr	880°C/6 hr	None
B4	1.75 : 2 : 1 : 2	760°C/3 hr	880°C/6 hr	300°C/O_2/70 hr
B5	1.85 : 2 : 1 : 2	760°C/3 hr	880°C/6 hr	300°C/O_2/70 hr
B6	2.00 : 2 : 1 : 2	760°C/3 hr	880°C/6 hr	300°C/O_2/70 hr

Tl-2201) and the total sintering time in the order of 10 hr result in a high degree of crystallinity and minimize the number of stacking faults in the material. Samples prepared at higher sintering temperatures normally show pronounced streaking effects in electron diffraction patterns which are indicative of stacking faults.

2.2. X-Ray Diffraction

Sample purity and lattice parameters were determined from Guinier film data using silicon (NBS 640b) as an internal standard. A computerized photoscanning system (55) in combination with programs for indexing and unit cell refinements was used for the extraction of lattice parameters (56).

2.3. Neutron Diffraction

Neutron powder diffraction data were collected at the pulsed neutron source ISIS, RAL, UK using the high flux, medium-resolution powder diffractometer POLARIS. A least-squares profile refinement program, TF12LS (57), based on the Rietveld technique (58) was used to analyze the TOF neutron powder diffraction data. Here, 4576 points were included in the refinements, covering a d-range from 0.5 to 3.0 Å. The scattering factors used were 0.8790 (Tl), 0.5250 (Ba), 0.7718 (Cu), 0.4900 (Ca), and 0.5805 (O) (59).

The refinements of Tl-2212 were carried out in space group $I4/mmm$ using the starting model derived by Cox *et al.* (36). In total, 24 variables were refined including scale factor (1), background parameters (5), profile parameters (2), and the structure parameters found in Table 5. Refinements of occupancy factors for Cu, Ba, O1, and O2 showed full occupancy within the standard deviations and were therefore fixed to 1.00. In the initial refinements the occupancy of the Ca site exceeded 1.00, which is explained by the fact that Tl is partly distributed at the Ca site. From ^{205}Tl NMR studies 5.3% of the total amount of Tl (obtained from gravimetry) was determined to occupy the Ca site (63, 68). Refinements of O3 in a 4*e* site

TABLE 3
Thallium Loss, Oxygen Uptake (Δox) and T_c for Tl-2201 with Different Thallium and Oxygen Content, with Estimated Errors for Δox in Parentheses

Sample	Tl-loss (%)	Δ ox	Symmetry	T_c (K)
A1, $Tl_{1.85}Ba_2CuO_{6-d}$	0.20	—	T	76
A2, $Tl_{1.95}Ba_2CuO_{6-d}$	0.31	—	O	76
A3, $Tl_{2.00}Ba_2CuO_{6-d}$	0.18	—	O	60
B1, $Tl_{1.85}Ba_2CuO_{6-d+\Delta ox}$	0.20	+0.017(5)	T	27
B2, $Tl_{1.95}Ba_2CuO_{6-d+\Delta ox}$	0.31	+0.043(5)	O	24
B3, $Tl_{2.00}Ba_2CuO_{6-d+\Delta ox}$	0.18	+0.072(5)	O	19

Note. Part of samples A1, A2, and A3 have been annealed in oxygen (300°C/70 hr). The annealed samples are denoted B1, B2, and B3, respectively (symmetry; T, tetragonal; O, othorhombic). Thallium loss and oxygen uptake are defined in Sections 3.1.1 and 3.1.2.

TABLE 4
Thallium Loss, Oxygen Uptake (Δox) and T_c for Tl-2212 with Different Thallium and Oxygen Content, with Estimated Errors for Δox in Parentheses

Sample	Tl-loss (%)	Δ ox	Symmetry	T_c (K)
A4, $Tl_{1.75}Ba_2CaCu_2O_{8-d}$	0.19	—	T	115
A5, $Tl_{1.85}Ba_2CaCu_2O_{8-d}$	0.23	—	T	114
A6, $Tl_{2.00}Ba_2CaCu_2O_{8-d}$	0.29	—	T	112
B4, $Tl_{1.75}Ba_2CaCu_2O_{8-d+\Delta ox}$	0.19	+0.157(5)	T	105
B5, $Tl_{1.85}Ba_2CaCu_2O_{8-d+\Delta ox}$	0.23	+0.225(5)	T	103
B6, $Tl_{2.00}Ba_2CaCu_2O_{8-d+\Delta ox}$	0.29	+0.165(5)	T	98

Note. Part of samples A4, A5, and A6 have been annealed in oxygen (300°C/70 hr). The annealed samples are denoted B4, B5, and B6, respectively (symmetry; T, tetragonal). Thallium loss and oxygen uptake are defined in Sections 3.1.1 and 3.1.2.

resulted in a large temperature factor, indicating disorder in the Tl_2O_4 layers. A displacement of O3 to the 16*n* site (x, $\frac{1}{2}$, z), a split site with occupancy $\frac{1}{4}$, gave a better fit with the data.

Tetragonal Tl-2201 data sets were refined in space group *I4/mmm* using a starting model derived by Torardi *et al.* (19). In total, 23 variables were varied with Tl, Ba, O2 at 4*e* sites (0, 0, z), Cu at a 2*b* site (0, 0, $\frac{1}{2}$), O1 at a 4*c* site (0, $\frac{1}{2}$, 0), and O3 at a 16*n* site (0, y, z). The disorder in the Tl_2O_4 layers is, as far as can be detected by the powder diffraction method, of the same type as that found in Tl-2212. In the final refinements isotropic temperature factors and the O3 occupancy factor were refined.

Orthorhombic Tl-2201 data sets were refined using the structure suggested by Parise *et al.* (40). All atomic positions in the orthorhombic model except O3 can be related to the tetragonal space group *I4/mmm*. The deviation of O3 from the 8*d* site (0, 0, z) can in the orthorhombic structure be described as a displacement along the *a*-axis of about 0.3 Å. The atomic positions used in the refinements are those summarized in Table 6.

2.4. T_c Measurements

The superconducting properties were studied by ac susceptibility measurements using a Quantum design SQUID magnetometer at temperatures down to 4 K in a field of 50 G.

3. RESULTS AND DISCUSSION

3.1. Structure and Properties

3.1.1. X-Ray Studies

The samples investigated were almost single phase irrespective of oxygen and thallium stoichiometry, the strongest $BaCuO_2$ peak being at a maximum in the order of 2–3% of the strongest peak in Tl-2201 or Tl-2212. For materials prepared as above, the solubility limit with respect to thallium is about $1.75 < 2-x < 2.00$. The amount of impurities ($BaCuO_2$) does not significantly change as thallium and/or oxygen content varies. We find no traces of the Tl-1201 and the Tl-1212 phases in our X-ray and neutron diffraction data. Furthermore, electron diffraction studies (54) show no signs of streaking. This indicates a well-crystallized material with a very limited amount of stacking faults.

3.1.1.1. The Tl-2201 system

The influence of thallium content.

An increase in thallium content is followed by an increase in *c*-axis length. A drastic increase in *c*-axis length precedes the tetragonal-to-orthorhombic phase transition in the oxygen-annealed samples (see Figs. 1 and 2). The discontinuous change in *c*-axis lengths, which is connected to the change in lattice symmetry, can only be detected in a series of materials prepared under conditions identical to those described in Section 2.1. These findings are supported by Raman studies where a discontinuous change in certain Raman mode frequencies precedes the tetragonal-to-orthorhombic phase transition and coincides with the change in *c*-axis lengths (60). A similar behavior, concerning the change in lattice symmetry and *c*-axis lengths, is found in $Tl_2Ba_{2-x}Sr_xCuO_{6-d}$ (53, 61) system which is tetragonal for $x > 0.50$ (see Fig. 3).

In Fig. 2 the *a* and *b* lattice parameters are plotted as a function of thallium content for two different oxygen contents. Thallium-deficient samples crystallize with tetragonal symmetry (*I4/mmm*), while the formation of the orthorhombic phase (*Abma*) is favored by high thallium content (see Table 6). A tetragonal sample with a nominal thallium composition of 1.850(4) was heated at 860°C for 3 hr in the presence of Tl_2O_3, using the same procedure as in sintering step 2, resulting in a transition to orthorhombic lattice symmetry. Together with the information in Table 3 it unambiguously shows the strong influence the thallium content has on the lattice symmetry. A high thallium con-

tent stabilizes the orthorhombic phase and causes a slight decrease in T_c.

The influence of oxygen content.

In Fig. 1 the lengths of the c-axes are plotted as a function of thallium content for Tl-2201 with two different oxygen contents. An increase in oxygen content causes a decrease in the c-axis length in agreement with earlier work (14, 31, 33, 62). In Fig. 4 the a and b lattice parameters are plotted as a function of Δ_{ox} in $Tl_{1.85}Ba_2CuO_{6-d+\Delta ox}$, which shows that a high oxygen content, obtained by annealing in oxygen, stabilizes the orthorhombic phase. In $Tl_2Ba_{2-x}La_xCuO_{6-d}$ ($0.00 < x < 0.30$) a higher lanthanum

TABLE 5

Cell Parameters (a, b, c, V), Atom Coordinates (x, y, z), Site Occupancies, and Isotropic Temperature Factors ($B = 8\ \pi^2 < u^2 > Å^2$) for $Tl_{1.85}Ba_2CaCu_2O_{8-d}$, $2 - x = 1.994$

		Sample	
		A6	B6
a (Å)		3.85582(5)	3.85385(4)
c (Å)		29.4089(7)	29.3169(6)
V (Å^3)		437.2	435.4
Tl			
$4e$ ($\frac{1}{2}$, $\frac{1}{2}$, z)	z	0.2131(1)	0.2134(1)
	n	0.997	0.997
	B	1.53(6)	1.76(5)
Ba			
$4e$ (0, 0, z)	z	0.1205(1)	0.1214(1)
	B	0.52(4)	0.56(3)
Ca			
$2a$ (0, 0, 0)	B	0.50(8)	0.66(5)
	n	1.03(3)	1.07(2)
Cu			
$4e$ ($\frac{1}{2}$, $\frac{1}{2}$, z)	z	0.0537(1)	0.0542(1)
	B	0.23(3)	0.26(3)
O(1)			
$8g$ (0, $\frac{1}{2}$, z)	z	0.0525(1)	0.0525(1)
	B	0.53(3)	0.51(3)
O(2)			
$4e$ ($\frac{1}{2}$, $\frac{1}{2}$, z)	z	0.1457(2)	0.1456(1)
	B	0.90(5)	0.93(4)
O(3)			
$16n$ (x, $\frac{1}{2}$, z)	x	0.5921(17)	0.6074(14)
	z	0.2816(2)	0.2824(3)
	n	0.230(6)	0.220(6)
	B	1.8(2)	2.2(2)
Observations		4396	4396
R_p (%)		6.32	5.58
R_{wp} (%)		3.35	1.60
R_{exp} (%)		2.58	1.22
χ^2		1.68	1.72

Note. The structures were refined in space group $I4/mmm$ (No. 139). Sample B6 is a part of sample A6 annealed in oxygen (see Table 2).

$R_p = (\Sigma(Y_i^{obs} - Y_i^{calc})/\Sigma Y_i^{obs})$, $R_{wp} = (\Sigma(Y_i^{obs} - Y_i^{calc})^2/\Sigma w_i(Y_i^{obs})^2)^{0.5}$, $R_{exp} = ((N - C + P)/\Sigma w_i(Y_i^{obs})^2)^{0.5}$, $\chi^2 = (R_{wp}/R_E)^2$.

TABLE 6

Cell Parameters (a, b, c, V), Atom Coordinates (x, y, z), Site Occupancies, and Isotropic Temperature Factors ($B = 8\ \pi^2 < u^2 > Å^2$) for $Tl_2Ba_2CuO_{6-d}$

		Sample	
		A3	B3
a (Å)		5.4881(2)	5.4847(2)
b (Å)		5.4532(2)	5.4420(2)
c (Å)		23.2159(6)	23.1598(7)
V (Å^3)		694.8	691.3
Tl			
$8d$ (0, 0, z)	z	0.2027(2)	0.2025(2)
	B	1.43(4)	1.49(4)
	n	0.998	0.998
Ba			
$8d$ (0, $\frac{1}{2}$, z)	z	0.0834(2)	0.0838(2)
	B	0.78(4)	0.93(5)
Cu			
$4a$ (0, 0, 0)	B	0.80(5)	0.95(6)
O(1)			
$8c$ ($\frac{3}{4}$, $\frac{1}{4}$, 0)	B	0.60(3)	0.63(4)
O(2)			
$8d$ (0, 0, z)	z	0.1171(2)	0.1173(2)
	B	0.85(4)	0.91(5)
O(3)			
$8f$ (x, 0, z)	x	0.058(1)	0.061(2)
	z	0.2903(4)	0.2912(4)
	B	2.6(2)	2.4(2)
	n	0.84(2)	0.78(2)
Observations		4576	4576
R_p (%)		7.22	7.64
R_{wp} (%)		2.11	4.00
R_{exp} (%)		1.53	2.73
χ^2		1.89	2.15

Note. The structures were refined in space group *Abma* (No. 64). Sample B3 is a part of sample A3 annealed in oxygen (see Table 1).

$R_p = (\Sigma(Y_i^{obs} - Y_i^{calc})/\Sigma Y_i^{obs})$, $R_{wp} = (\Sigma(Y_i^{obs} - Y_i^{calc})^2/\Sigma w_i(Y_i^{obs})^2)^{0.5}$, $R_{exp} = ((N - C + P)/\Sigma w_i(Y_i^{obs})^2)^{0.5}$, $\chi^2 = (R_{wp}/R_E)^2$.

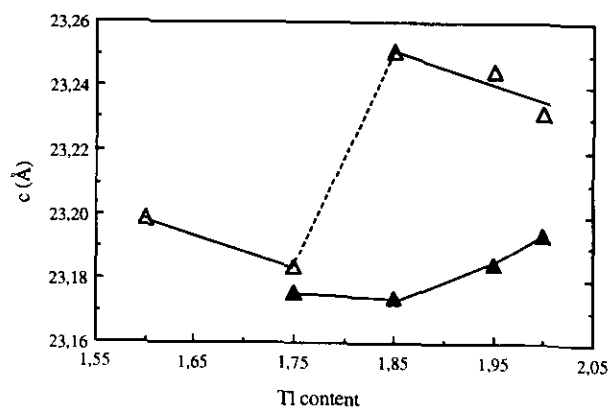

FIG. 1. c-axis length as a function of thallium content for Tl-2201 at two different oxygen contents. Open and closed triangles refer to series A and B samples, respectively. The series B samples are the ones with high oxygen content (Table 1).

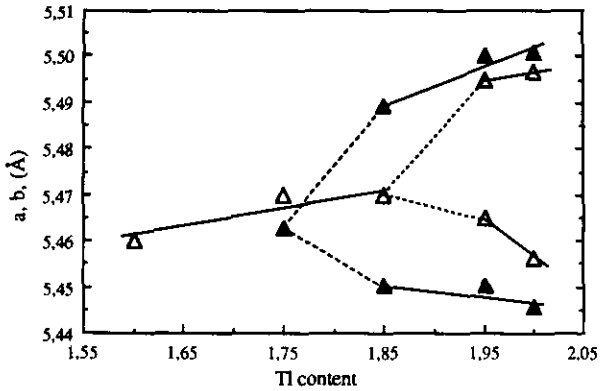

FIG. 2. Lattice parameters a and b as a function of thallium content for Tl-2201 (Guinier data; $0.0003 < \sigma < 0.0007$). In the tetragonal region, the a-axis has been plotted as a $\sqrt{2}$. Open triangles denote the as-prepared samples (series A) and closed triangles denote the oxygen-annealed samples (series B) with higher oxygen content (Table 1).

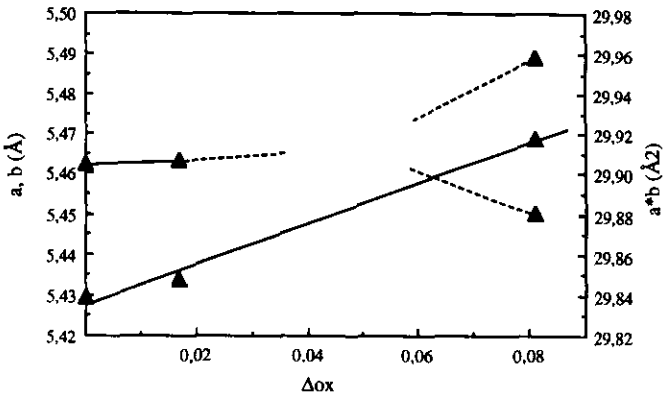

FIG. 4. The a and b lattice parameters as a function of oxygen content in $Tl_{1.85}Ba_2CuO_{6-d+\Delta ox}$.

leads to an increased difference in the a and b lattice parameters (23).

It is shown that an increase in oxygen content causes a pronounced decrease in T_c (Table 3). The oxygen uptake in the Tl-2201 system shows an increase with growing thallium content, and the sample can be overdoped by introducing too much oxygen (30, 43, 44). As a result T_c decreases or even vanishes. Samples with high oxygen content can be improved with respect to T_c when reduced in a H_2/Ar atmosphere, i.e., the change in oxygen content seems to be reversible (32). There is, however, the possibility that hydrogen enters the structure as in Tl-2212 (63).

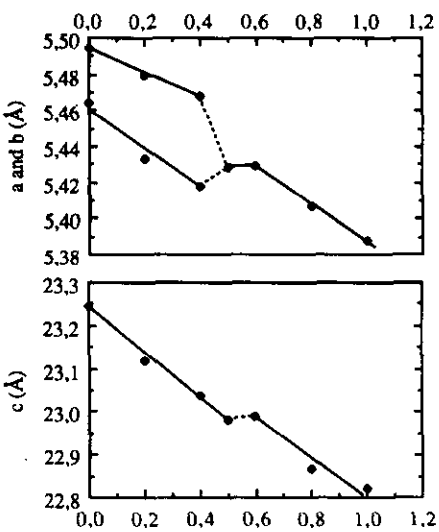

FIG. 3. The a, b, and c lattice parameters as a function of strontium content in $Tl_2Ba_{2-x}Sr_xCuO_{-d}$.

3.1.1.2. The Tl-2212 system.

Tl-2212 shows a slight decrease in c-axis length with an increase in thallium content (Fig. 5). There is no sign of a discontinuous change as in the Tl-2201 system, which we relate to the observation that the lattice symmetry does not change with thallium or oxygen stoichiometry. The structure shows tetragonal symmetry (*I4/mmm*) for all compositions investigated in this study. Deviations from tetragonal symmetry at a local level has, however, been reported in the literature (64–67).

In Table 4 the weight change upon annealing in oxygen is summarized for Tl-2212 samples together with corresponding T_c values. The oxygen stoichiometry is again the main factor in determining the superconducting properties of Tl-2212, though not as much as in Tl-2201 (32, 33).

3.1.2. Neutron Diffraction Studies

In Figs. 6a, 6b, and 6c representative neutron powder diffraction patterns of tetragonal and orthorhombic Tl-2201 as well as tetragonal Tl-2212 are shown. In Tables

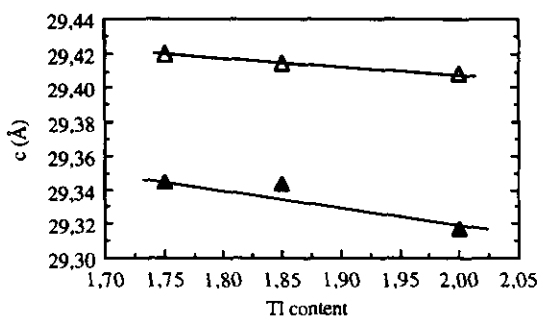

FIG. 5. c-axis length as a function of thallium content for Tl-2212 at two different oxygen contents. Open and closed triangles refer to series A and B samples, respectively. The series B samples have the highest oxygen content (see Table 2).

TABLE 7
A Change in Cu–O Coordination upon Oxygen Annealing for the Tl-2212 Structure

	1.75		1.85		2.00	
Tl_{2-x} Ox. cont.	A4 $8-d$	B4 $8-d+\Delta ox$	A5 $8-d$	B5 $8-d+\Delta ox$	A6 $8-d$	B6 $8-d+\Delta ox$
Cu–O1	1.9266(1)	1.9270(1)	1.9268(1)	1.9281(1)	1.9282(1)	1.9276(1)
Cu–O2	2.727(4)	2.672(4)	2.712(4)	2.670(4)	2.706(4)	2.680(3)
Cu–O2/CuO1	1.415	1.387	1.408	1.385	1.403	1.390

Note. The B series samples contain more oxygen than the A series samples. Distances are given in (Å).

5 and 6 crystallographic information is presented for two Tl-2201 samples and two Tl-2212 samples with low and high oxygen content, respectively. The findings are in agreement with earlier neutron structure determinations. The difference in oxygen content in samples A and B, respectively, is below the significance level, at least not reflected in n_{03}. The only way to explain the increase in weight during annealing is by an uptake of oxygen as discussed in Section 2.1.

3.1.2.1. The Tl-2212 system.

In Table 7 the change in Cu–O coordination upon oxygen annealing is summarized for the Tl-2212 system. The coordination polyhedron of copper is actually slightly compressed along the z-direction with an increase in oxygen content. The change in metal-to-apex oxygen distances in the z-direction shows the same behavior as the copper-to-apex oxygen distances in Y-123, i.e., the Tl–O2 distance increases and the Cu–O2 distance decreases. Thus the shortening of the c-axis length is to a large extent due to a change in Cu–O coordination.

In Figs. 7a and 7b the close resemblance between the Tl-2212 and Y-123 structures, and their response to an increase in oxygen content is shown. In the former compound the Tl_2O_4 layers act as charge reservoirs and in the Y-123 structure the CuO_x chains play a similar role. Table 8 shows a summary of relevant interatomic distances for Tl-2212. In oxygen-annealed samples the barium and the apex oxygen (O2) atoms move in opposite directions, Ba moving toward the Tl_2O_4 layers and O2 toward the CuO_2 plane, resulting in a decrease in the $\Delta(Ba–O2)_z$ distance by 0.03 Å (see Fig. 7a).[2] Moreover, the puckering of the CuO_2 plane increases as the Cu atom is further displaced out of the plane and the Cu–Cu interlayer distance increase by 0.03 Å. All these changes, in c-axis length and in relative atomic positions, are reminiscent of those in the Y-123 system.[3] A decrease in the intralayer Tl–Tl distance, $(Tl–Tl)_z$, takes place which has been proposed to be a sign of a reduction of the Tl_2O_4 substructure, i.e., an oxidation of the CuO_2 layer (14). The Tl-2212 there is a decrease in T_c with growing oxygen content, which means that the as-prepared materials already are in the overdoped region in the phase diagram. This has been confirmed by solid state NMR studies (63, 68). The ^{205}Tl NMR Knight shift is strongly dependent on the oxygen content and gives a measure of the hole concentration in the CuO_2 planes.

In Figure 7b the corresponding structural changes are indicated for Y-123 and they can be explained by an increase in positive charge carrier concentration in the CuO_2 planes (69–71). A shift of the Ba^{2+} toward the CuO_3 chains, a displacement of O4 in the opposite direction and a depuckering of the CuO_2 planes occur. The change in $\Delta(Cu–O2, 3)_z$ and $\Delta(Ba–O4)_z$[4] is the strongest structural indication of a charge transfer in the Y-123 system. A decrease in oxygen content and also Me^{3+} doping (Co^{3+}, Al^{3+}, Fe^{3+}) at the Cu site causes similar changes in the structure and thus in charge distribution and T_c. From Raman scattering studies it has been shown that the O4 vibration frequency scales with T_c in a similar way in the two cases, indicating the importance of charge transfer and the close resemblance between oxygen-deficient and Me^{3+}-doped materials (72–72, 76–79).

3.1.2.2. Comparison of Tl-2201 and Tl-2212.

In Table 9 various atomic distances are summarized for the Tl-2201 system. The structural changes induced by a change in thallium and oxygen content are similar to the

[2] $\Delta(Ba–O2)_z$ and $\Delta(Cu–O1)_z$ denote the distances between layers formed by Ba and O2, and Cu and O1 atoms, respectively, in the Tl-2212 structure.

[3] $\Delta(Cu–O2,3)_z$ and $\Delta(Ba–O4)_z$ denote the distances between layers formed by Cu2 and O2, O3 atoms, and Ba and O4 atoms, respectively. They are the equivalents of $\Delta(Cu–O1)_z$ and $\Delta(Ba–O2)_z$ in the Tl-2212 system.

[4] Although the changes are small we have confidence in their reliability as the neutron data obtained at POLARIS, ISIS, RAL, UK are of high quality. Series of samples investigated always show clear trends in e.g., bond distance changes with minor changes in composition (23, 53, 61, 72–75).

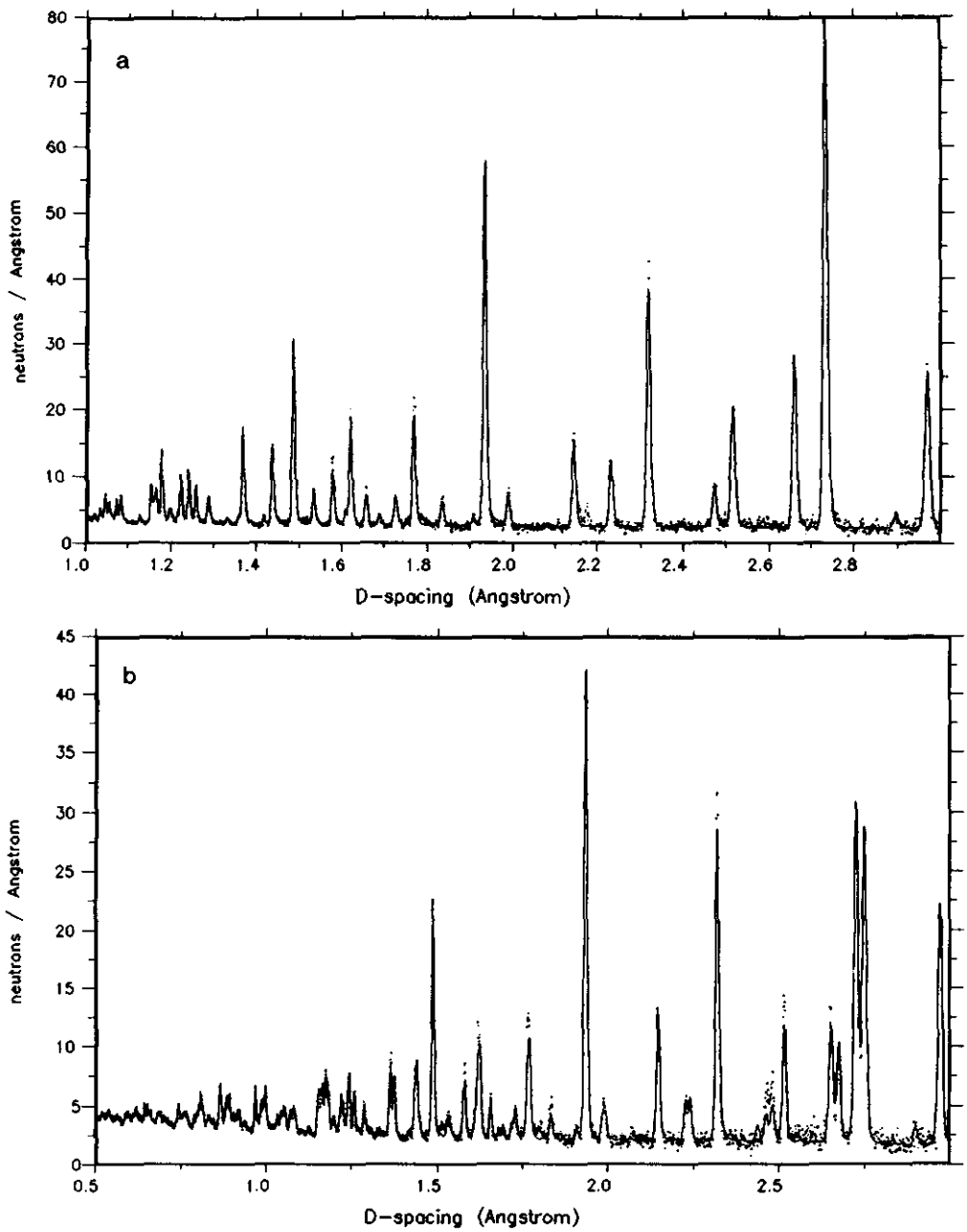

FIG. 6. Final fit of the Rietveld refined data for (a) tetragonal Tl-2201 (sample B1), (b) orthorhombic Tl-2201 (sample B2), and (c) Tl-2212 (sample B6). Dots are experimental points and the solid line refers to the calculated pattern. The profiles of the tetragonal samples show weak peaks at 2.09 (sample B1), 1.76, 2.15, 2.42, and 2.54 Å (sample B6) which were not possible to refine with the models used.

changes occurring in the Tl-2212 system. However, in Tl-2201 the structure of the CuO_2 layer is planar by crystallographic reasons. The puckering of the CuO_2 plane therefore cannot be used as a probe for charge redistribution in Tl-2201. The decrease in the $\Delta(Ba–O2)_z$ distance is indicative of an increase in charge carrier concentration in the CuO_2 planes and in Tl-2201 (the distance is defined as for Tl-2212). A change in oxygen content causes a similar change in the average atomic structure of the Tl_2O_4 layer in both systems. This may indicate that the energy of the Tl 6*s* bands and thus its overlap with the Cu-*d* bands are altered in much the same way in the two systems.

Due to the disorder in the Tl_2O_4 layers it is difficult to obtain an accurate estimate of the thallium and oxygen occupancies from the Rietveld refinements of neutron powder diffraction data. In a neutron diffraction study on the $Tl_2Ba_{2-x}Sr_xCu_2O_{6-d}$ system the oxygen content was refined to about 5.55–5.60 for four different values of x

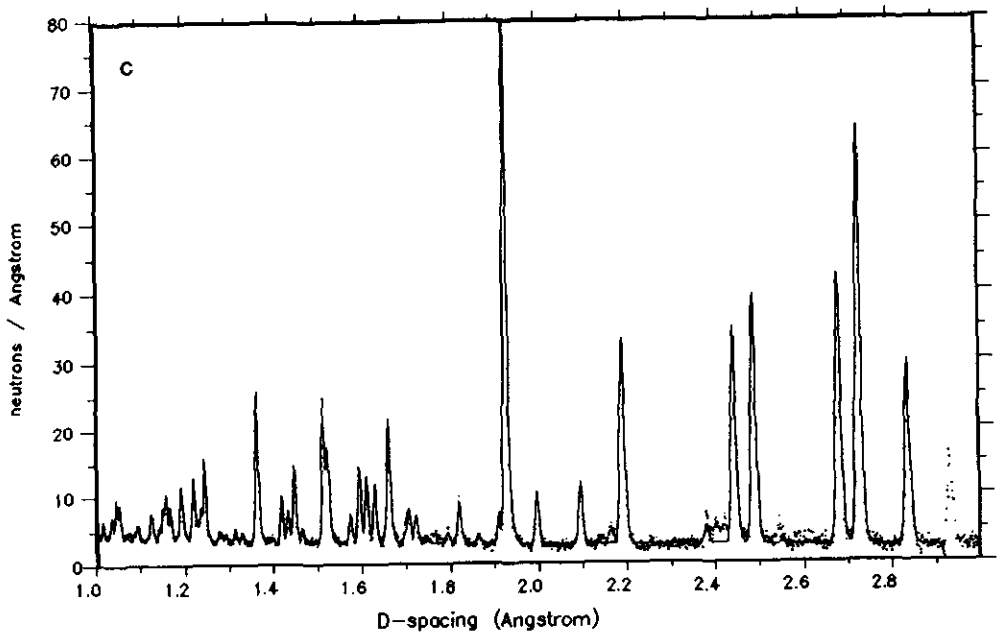

FIG. 6—*Continued*

(53, 61), and one may assume the oxygen content in the series A samples to be 5.6 or at least well below 6. In a similar study performed on the Tl-2212 system the oxygen occupancies were refined to about 7.8 for samples with different strontium content (80), compared to 7.9 in this study. We found no evidence of oxygen atoms occupying interstitial sites as suggested by Shimakawa (26). Rietveld analysis indicates that the thallium vacancies in thallium-deficient Tl-2201 and Tl-2212 are statistically distributed in the Tl_2O_4 layers. In a recent work the same has been concluded for the Tl-2212 structure (29). The Penn State group has, from Monte Carlo simulations and PDF analysis of Tl-2212, proposed some more detailed models (64–67). They have found that Tl as well as O3 atoms are displaced from the high symmetry crystallographic positions in a way to build up zig-zag Tl chains. A pronounced change in local order, in particular of the oxygen atoms around Cu, has been monitored at the onset of superconductivity (65–67). The ordering is, however, short range and therefore not observed by conventional crystallographic methods.

CONCLUSION

By use of an optimized preparative method thallium cuprate superconductors with a well-defined thallium content can be prepared in a controlled and reproducible way. The thallium loss is well below 0.5% in the preparation and of the same size for different batches.

The orthorhombic-to-tetragonal phase transition is

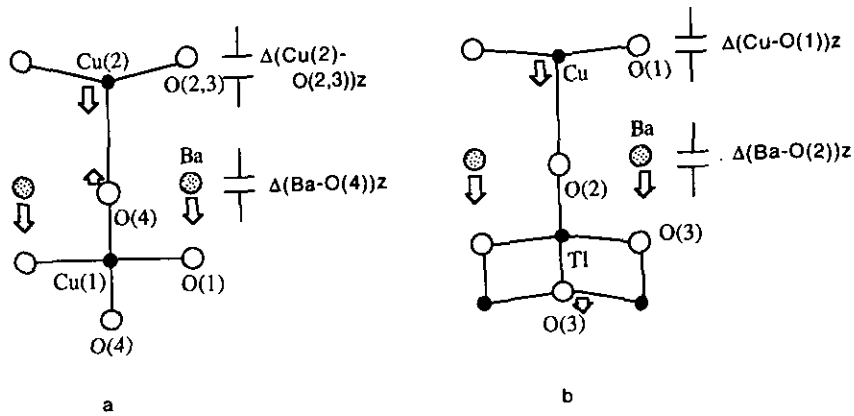

FIG. 7. Atomic displacements caused by an increased charge carrier concentration in the CuO_2 planes in (a) Y-123 and (b) Tl-2212, respectively.

TABLE 8
A Summary of Some Interatomic Distances (Å) for Tl-2212 Samples with Different Thallium and Oxygen Content

	1.75		1.85		2.00	
Tl_{2-x}	A4	B4	A5	B5	A6	B6
Tl–O2	1.983(4)	1.984(5)	1.977(4)	1.992(5)	1.982(4)	1.988(4)
Cu–O2	2.727(4)	2.672(4)	2.712(3)	2.670(4)	2.706(4)	2.680(3)
Δ(Cu–Cu)z	3.160(2)	3.183(3)	3.153(2)	3.187(3)	3.158(3)	3.178(2)
Δ(Cu–O1)z	0.035	0.059	0.026	0.059	0.035	0.050
Δ(Ba–O2)z	0.715	0.684	0.753	0.704	0.753	0.710
Δ(Tl–Tl)z	2.206	2.189	2.177	2.160	2.170	2.146
Δ(O3–O3)z	1.871	1.919	1.830	1.913	1.859	1.900
Δ(Tl–O3)z	0.168	0.135	0.173	0.123	0.156	0.123

Note. The B series samples are the ones with high oxygen content.

TABLE 9
A Summary of Some Interatomic Distances for Tl-2201 Samples with Different Thallium and Oxygen Content

	1.85		1.95		2.00	
Tl_{2-x}	A1	B1	A2	B2	A3	B3
Tl–O2	1.986	1.983	1.983	1.985	1.990	1.973
Cu–O2	2.722	2.715	2.722	2.713	2.719	2.716
Δ(Ba–O2)z	0.792	0.769	0.790	0.768	0.782	0.776
Δ(Tl–Tl)z	2.197	2.187	2.202	2.198	2.196	2.200
Δ(O3–O3)z	1.812	1.835	1.867	1.901	1.871	1.908
Δ(Tl–O3)z	0.193	0.176	0.167	0.148	0.162	0.146

Note. The B series samples are the ones with high oxygen content.

mainly controlled by the thallium content, and samples with a thallium content, $2\text{-}x < 1.86$, crystallize in tetragonal form. The oxygen content does, however, to a minor extent increase the stability range of the orhorhombic phase toward slightly lower values of $2 - x$.

A discontinuous change in c-axis length precedes the phase transition from tetragonal-to-orthorhombic symmetry in Tl-2201 inrrespective of whether the transition is caused by a change in thallium content or by strontium substitution at the Ba site.

It is shown that orthorhombic as well as tetragonal Tl-2201 can be made superconducting by varying thallium and oxygen content in an appropriate way. The thallium content is the main factor in determining lattice symmetry, while the oxygen content has a stronger influence on T_c, the latter statement also being valid for the Tl-2212 system. In both systems a decrease in oxygen content leads to an increase in T_c, indicating that all the materials investigated in this study are in the overdoped region of the phase diagram.

Concerning the Tl-2212 system the change in T_c as a function of oxygen content can be correlated to a change in relative atomic positions indicative of a charge redistribution. This is in analogy with findings for the Y-123 system.

ACKNOWLEDGMENTS

Many thanks are due Steve Hull at ISIS, Rutherford-Appleton Laboratories, for his skillful assistance in the collection of neutron diffraction data as well as for making the stay at ISIS easy going and pleasant. The authors are also indebted to Norbert Winzek and Michael Mehring, Universität Stuttgart, for access to results prior to publication. This work was financially supported by the Swedish National Research Council and the Swedish Board for Technical Development. One of the authors (S.-G. E.) is also grateful for support from The Swedish Institute, the Max-Planck Gesellschaft, and Adlerbertska Forskningsfonden during his stay at MPI für Festkörperforschung, Stuttgart.

REFERENCES

1. B. Raveau, C. Michel, M. Hervieu, D. Groult, and J. Provost, *J. Solid State Chem.* **85,** 181 (1988).

2. B. Raveau, C. Michel, and M. Hervieu, *J. Solid State Chem.* **88,** 140 (1990).
3. M. W. Shafer and T. Penney, *Eur. J. Solid State Inorg. Chem.* **27,** 191 (1990).
4. H. F. Poulsen, N. H. Andersen, J. V. Andersen, H. Bohr, and O. G. Mouritsen, *Nature* **349,** 594 (1991).
5. H. F. Poulsen, N. H. Andersen, J. V. Andersen, H. Bohr, and O. G. Mouritsen, *Phys. Rev. Lett.* **66,** 465 (1991).
6. S. Pekker, A. Janossy, and A. Rockenbauer, *Physica C* **181,** 11 (1991).
7. J. D. Jorgensen, S. Pei, P. Lightfoot, H. Shi, A. P. Paulikas, and B. W. Veal, *Physica C* **167,** 371 (1990).
8. B. W. Veal, A. P. Paulikas, H. You, H. Shi, Y. Fang, and J. W. Downey, *Phys. Rev. B* **42,** 6305 (1990).
9. B. W. Veal and A. P. Paulikas, *Physica C* **184,** 321 (1991).
10. Z. Z. Sheng and A. M. Hermann, *Nature* **332,** 55 (1988).
11. Z. Z. Sheng and A. M. Hermann, *Nature* **332,** 138 (1988).
12. M. Hervieu, C. Michel, A. Maignan, C. Martin, and B. Raveau, *J. Solid State Chem.* **74,** 3428 (1988).
13. S. S. P. Parkin, V. Y. Lee, E. M. Engler, A. I. Nazzal, T. C. Huang, G. Gorman, R. Savoy, and R. Beyers, *Phys. Rev. Lett.* **60,** 2539 (1988).
14. Y. Shimakawa, Y. Kubo, T. Manako, H. Igarashi, F. Izumi, and A. Asano, *Phys. Rev. B* **42,** 10165 (1990).
15. A. W. Hewat, P. Bordet, J. J. Capponi, C. Chaillout, J. Chenevas, M. Godinho, E. A. Hewat, J. L. Hodeau, and M. Marezio, *Physica C* **156,** 369 (1988).
16. R. Beyers, S. S. P. Parkin, V. Y. Lee, A. I. Nazzal, R. Savoy, G. Gorman, T. C. Huang, and S. Laplaca, *Appl. Phys. Lett.* **53,** 432 (1988).
17. A. Maignan, C. Michel, M. Hervieu, C. Martin, D. Groult, and B. Raveau, *Mod. Phys. Lett. B* **2,** 681 (1988).
18. B. Morosin, D. S. Ginsley, E. L. Venturini, P. F. Hlava, R. J. Baughman, J. F. Kwak, and J. E. Schirber, *Physica C* **152,** 223 (1988).
19. C. C. Torardi, M. A. Subramanian, J. C. Calabrese, J. Gopalakrishnan, E. M. McCarron, K. J. Morrissey, T. R. Askew, R. B. Flippen, U. Chowdhry, and A. W. Sleight, *Phys. Rev. B* **38,** 225 (1988).
20. Y. Shimakawa, Y. Kubo, T. Manako, Y. Nakabayashi, and H. Igarashi, *Physica C* **156,** 97 (1988).
21. T. C. Huang, V. Y. Lee, R. Karimi, R. Beyers, and S. S. P. Parkin, *Mater. Res. Bull.* **23,** 1307 (1988).
22. K. K. Saini, C. P. Sharma, S. N. Ekbote, D. K. Suri, P. Asthana, K. C. Nagpai, C. Chandra, and S. Chandra, *Solid State Commun.* **74,** 789 (1990).
23. C. Ström, M. Käll, L.-G. Johansson, S.-G. Eriksson, and L. Börjesson, *Physica C* **185–189,** 625 (1991).
24. B. Raveau, C. Michel, M. Hervieu, D. Groult, C. Martin, A. Maignan, and J. Provost, *Physica C* **190,** 1 (1991).
25. C. Ström, S.-G. Eriksson, L.-G. Johansson, and A. Simon *in* "Conference Proceeding, Accuracy in Powder Diffraction II," May 26–29, 1992. Gaithersburg, USA.
26. Y. Shimakawa, Y. Kubo, T. Manako, and H. Igarashi, *Phys. Rev. B* **40,** 11400 (1989).
27. B. Morosin, R. J. Baughman, D. S. Ginley, J. E. Schirber, and E. L. Venturini, *Physica C* **165,** 115 (1990).
28. B. Morosin, D. S. Ginley, E. L. Venturini, R. J. Baughman, and C. P. Tigges, *Physica C* **172,** 413 (1991).
29. C. Michel, C. Martin, M. Hervieu, A. Maignan, J. Provost, M. Huve, and B. Raveau, *J. Solid State Chem.* **96,** 271 (1992).
30. D. Jung, M.-H. Whangboo, M. Herron, and C. C. Torardi, *Physica C* **160,** 381 (1989).
31. K. W. Ramanujachary, S. Li, and M. Greenblatt, *Physica C* **165,** 377 (1990).
32. C. Martin, A. Maignan, J. Provost, C. Michel, M. Hervieu, R. Tournier, and B. Raveau, *Physica C* **168,** 8 (1990).
33. A. Maignan, C. Martin, M. Huve, J. Provost, M. Hervieu, C. Michel, and B. Raveau, *Physica C* **170,** 350 (1990).
34. C. Ström, S.-G. Eriksson, L.-G. Johansson, and A. Simon, *in* "Conference Proceeding, Joint Nordic Spring Meeting 92," May 7–10, 1992. Nyborg, Denmark.
35. E. A. Hewat, P. Bordet, J. J. Capponi, C. Chaillout, J. Chenevas, M. Godinho, A. W. Hewat, J. L. Hodeau, and M. Marezio, *Physica C* **156,** 375 (1988).
36. D. E. Cox, C. C. Torardi, M. A. Subramanian, J. Gopalakrishnan, and A. W. Sleight, *Phys. Rev. B* **38,** 6624 (1988).
37. S. J. Hibble, A. K. Cheetham, A. M. Chippindale, P. Day, and J. A. Hriljac, *Physica C* **156,** 604 (1988).
38. T. Zetterer, H. H. Otto, G. Lugert, and K. F. Renk, *Z. Phys. B* **73,** 321 (1988).
39. J. B. Parise, N. Herron, M. K. Crawford, and P. L. Gai, *Physica C* **159,** 255 (1989).
40. J. B. Parise, C. C. Torardi, M. A. Subramanian, J. Gopalakrishnan, and A. W. Sleight, *Physica C* **159,** 239 (1989).
41. D. M. Deleeuw, W. A. Groen, J. C. Jol, H. B. Brom, and H. W. Zandbergen, *Physica C* **166,** 349 (1990).
42. M. Paranthaman, A. Manthiram, and J. B. Goodenough, *J. Solid State Chem.* **87,** 479 (1990).
43. M.-H. Whangboo, D. B. Kang, and C. C. Torardi, *Physica C* **158,** 371 (1989).
44. A. Manthiram, M. Paranthaman, and J. B. Goodenough, *Physica C* **171,** 135 (1990).
45. D. R. Hamman and L. F. Mattheiss, *Phys. Rev. B* **38,** 5138 (1988).
46. T. Suzuki, M. Nagoshi, Y. Fukuda, Y. Syono, M. Kkuchi, N. Kobayashi, and M. Tachiki, *Phys. Rev. B* **40,** 5184 (1988).
47. C. C. Torardi, M. A. Subramanian, J. C. Calabrese, J. Gopalakrishnan, K. J. Morrissey, T. R. Askew, R. B. Flippen, U. Chowdhry, and A. W. Sleight, *Science* **240,** 631 (1988).
48. M. A. Subramanian, J. C. Calabrese, C. C. Torardi, J. Gopalakrishnan, T. R. Askew, R. B. Flippen, K. J. Morrissey, U. Chowdhry, and A. W. Sleight, *Nature* **332,** 420 (1988).
49. F. Hentsch, N. Winzek, M. Mehring, H. J. Mattausch, and A. Simon, *Physica C* **158,** 137 (1989).
50. J. Gopalakrishnan, R. Vijayaraghavan, R. Nagarajan, and C. Shivankumara, *J. Solid State Chem.* **93,** 272 (1991).
51. A. Manthiram, M. Paranthaman, and J. B. Goodenough, *J. Solid State Chem.* **96,** 464 (1992).
52. J. Gopalakrishnan, R. Vijayaraghavan, R. Nagarajan, and C. Shivakumara, *J. Solid State Chem.* **96,** 468 (1992).
53. C. Ström, M. Käll, L.-G. Johansson, S.-G. Eriksson, and L. Börjesson, *Physica C* **185–189,** 623 (1991).
54. L.-G. Johansson, C. Ström, S.-G. Eriksson, and I. Bryntse, *Physica C,* accepted for publication.
55. K. E. Johansson, T. Palm, and P.-E. Werner, *J. Phys. E* **13,** 1289 (1980).
56. P.-E. Werner, *Ark. Kemi* **31,** 513 (1969).
57. W. I. F. David, RAL Report, RAL 88-103 (1988).
58. H. M. Rietveld, *J. Appl. Crystallogr.* **2,** 65 (1969).
59. S. W. Lovesey, "Theory of Neutron Scattering from Condensed Matter," Vol. 1, International Series of Monographs on Physics, Vol. 72. (1984).
60. M. Käll, L. Börjesson, C. Ström, S.-G. Eriksson, and L.-G. Johansson, submitted for publication.
61. C. Ström, S.-G. Eriksson, and L.-G. Johansson, *Physica C,* in press.
62. J. B. Parise, J. Gopalakrishnan, M. A. Subramanian, and A. W. Sleight, *J. Solid State Chem.* **76,** 432 (1988).
63. N. Winzek, private communication.
64. W. Dmowski, B. H. Toby, T. Egami, M. A. Subramanian, J. Gopalakrishnan, and A. W. Sleight, *Phys. Rev. Lett.* **61,** 2608 (1988).

65. B. H. Toby, T. Egami, J. D. Jorgensen, and M. A. Subramanian, *Phys. Rev. Lett.* **64,** 2414 (1990).
66. T. Egami, B. H. Toby, S. J. L. Billinge, H. D. Rosenfeld, J. D. Jorgensen, D. G. Hinks, B. Dabrowski, M. A. Subramanian, M. K. Crawford, W. E. Farneth, and E. M. McCarron, *Physica C* **185–189,** 867 (1991).
67. T. Egami, B. H. Toby, S. J. L. Billinge, C. Janot, J. D. Jorgensen, D. G. Hinks, M. A. Subramanian, M. K. Crawford, W. E. Farneth, and E. M. McCarron, "High Temperature Superconductivity; Physical Properties, Microscopic Theory and Mechanisms," p. 389. Plenum, 1991.
68. N. Winzek, H. J. Mattausch, S.-G. Eriksson, C. Ström, R. K. Kremer, and A. Simon, *Physica C* **205,** 45 (1993).
69. J. D. Jorgensen, B. W. Veal, A. P. Paulikas, L. J. Nowicki, G. W. Crabtree, H. Claus, and W. K. Kwok, *Phys. Rev. B* **41,** 1863 (1990).
70. A. Furrer, P. Allenspach, J. Mesot, U. Staub, H. Blank, H. Mutka, C. Vettier, E. Kaldis, J. Karpinski, S. Rusiecki, and A. Mirmelstein, *Eur. J. Solid State Inorg. Chem.* **28,** 627 (1991).
71. Z. Z. Wang, J. Clayhold, N. P. Ong, J. M. Tarascon, L. H. Greene, W. R. McKinnon, and G. W. Hull, *Phys. Rev. B* **36,** 7222 (1987).
72. S.-G. Eriksson, thesis. University of Göteborg, Sweden, 1990.
73. M. Kakihana, S.-G. Eriksson, L. Börjesson, L.-G. Johansson, and C. Ström, *Phys. Rev. B* **47,** 5359 (1993).
74. S.-G. Eriksson, L.-G. Johansson, C. Ström, P. Berastegui, L. Börjesson, M. Käll, and M. Kakihana, *Physica C* **185–189,** 893 (1991).
75. S.-G. Eriksson, C. Ström, and M. Kakihana, submitted for publication.
76. R. Sonntag, D. Hohlwein, A. Hoser, A. Prandl, W. Schäfer, R. Kiemel, S. Kemmler-Sack, S. Lösch, and M. Schlichenmaier, *Physica C* **159,** 141 (1989).
77. P. F. Miceli, J. M. Tarascon, L. H. Greene, P. Barboux, F. J. Rotella, and J. D. Jorgensen, *Phys. Rev. B* **37,** 5932 (1988).
78. M. Kakihana, L. Börjesson, S.-G. Eriksson, P. Svedlindh, and P. Norling, *Phys. Rev. B* **40,** 6787 (1989).
79. C. Thomsen, R. Liu, M. Bauer, A. Wittlin, L. Genzel, M. Cardona, E. Schönherr, W. Bauhofer, and W. König, *Solid State Commun.* **65,** 55 (1988).
80. C. Ström, L.-G. Johansson, and S.-G. Eriksson, unpublished results.